

Article

Maintenance of the Metastable State and Induced Precipitation of Dissolved Neodymium (III) in an Na₂CO₃ Solution

Youming Yang^{1,2}, Xiaolin Zhang¹, Kaizhong Li^{1,*} , Li Wang³, Fei Niu^{1,2}, Donghui Liu¹ and Yuning Meng¹

¹ Faculty of Materials Metallurgy and Chemistry, Jiangxi University of Science and Technology, Ganzhou 341000, China; Yanguming@126.com (Y.Y.); userlin116@126.com (X.Z.); niufeiixust@foxmail.com (F.N.); Fiboy@163.com (D.L.); ynmeng88@126.com (Y.M.)

² Institute of Engineering Research, Jiangxi University of Science and Technology, Ganzhou 341000, China

³ College of Vanadium and Titanium, Panzhihua University, Panzhihua 617000, China; wl003@126.com

* Correspondence: likaizhong1105@163.com

Abstract: Rare earths dissolved in carbonate solutions exhibit a metastable state. During the period of metastability, rare earths dissolve stably without precipitation. In this paper, neodymium was chosen as a representative rare earth element. The effects of additional NaCl and CO₂ on the metastable state were investigated. The metastable state can be controlled by adding NaCl to the Na₂CO₃ solution. Molecular dynamics studies indicated that the Cl⁻ provided by the additional NaCl partially occupied the coordination layer of Nd³⁺, causing the delayed formation of neodymium carbonate precipitation. In addition, the additional NaCl decreased the concentration of free carbonate in the solution, thereby reducing the behavior of free contact between carbonate and Nd, as well as resulting in the delay of Nd precipitate formation. Consequently, the period of the metastable state was prolonged in the case of introduction of NaCl. However, changing the solution environment by introducing CO₂ can destroy the metastable state rapidly. Introduction of CO₂ gas significantly decreased the CO₃²⁻ content in the solution and increased its activity, resulting in an increase of the free CO₃²⁻ concentration of the solution in the opposite direction. As a result, the precipitation process was accelerated and the metastable state was destroyed. It was possible to obtain a large amount of rare earth carbonate precipitation in a short term by introducing CO₂ into the solution with dissolved rare earths in the metastable state to achieve rapid separation of rare earths without introducing other precipitants during the process.

Keywords: neodymium; metastable state; maintenance; induced precipitation



Citation: Yang, Y.; Zhang, X.; Li, K.; Wang, L.; Niu, F.; Liu, D.; Meng, Y. Maintenance of the Metastable State and Induced Precipitation of Dissolved Neodymium (III) in an Na₂CO₃ Solution. *Minerals* **2021**, *11*, 952. <https://doi.org/10.3390/min11090952>

Academic Editors: Shuai Wang, Xingjie Wang, Jia Yang and Kenneth N. Han

Received: 19 July 2021

Accepted: 27 August 2021

Published: 31 August 2021

Publisher's Note: MDPI stays neutral with regard to jurisdictional claims in published maps and institutional affiliations.



Copyright: © 2021 by the authors. Licensee MDPI, Basel, Switzerland. This article is an open access article distributed under the terms and conditions of the Creative Commons Attribution (CC BY) license (<https://creativecommons.org/licenses/by/4.0/>).

1. Introduction

Rare earths are strategic metal resources that are used in a wide range of industries. For example, they can be found in the development of high-tech advanced materials for permanent magnets, luminescence, catalysis and hydrogen storage, as well as in basic industries such as metallurgy, machinery and petrochemicals in general [1–5].

Rare earth carbonate is a barely soluble substance, with a solubility in water of only 10⁻⁵–10⁻⁷ mol·L⁻¹ [6,7]. However, when rare earth ions are added to a higher concentration of alkali metal carbonate solution, there occurs the phenomenon of rare earth dissolution in the carbonate solution. The amount of rare earth dissolution increases with increased carbonate concentration. As early as 1963, Taketatsu [8,9] found that when a certain amount of rare earth chloride solution was gradually added to a concentrated K₂CO₃ solution, sediment of the rare earth carbonate was generated first and then dissolved again with the passage of reaction time. The dissolution amount of rare earth increased with the increase of CO₃²⁻ concentration and the atomic number of the rare earth (except for Ce and Y). Restricted by the situation of the industry at that time, rare earth resources were not as scarce as nowadays, but comparatively abundant. Therefore, the discovery of

the regularity of dissolution of rare earths in carbonate solution did not attract the attention of the rare earth separation industry.

Vasconcellos et al. [10] carried out a feasibility study on selective dissolution, separation and enrichment of a rare earth in carbonate solution based on Taketatsu's regularity [8,9]. Low-Ce rare earth carbonate concentrates were selectively dissolved and successfully enriched with yttrium by using $\text{NH}_4\text{HCO}_3/(\text{NH}_4)_2\text{CO}_3$ solution as a carrier. The grade of yttrium increased from 2.4% to 81.0%. In addition, it was also found that the concentration of NH_4^+ influenced the dissolution behavior of rare earth in the solution system in that a higher concentration of NH_4^+ could enhance the solubility of rare earths. Reference to research on the equilibrium hydrochemical behavior of neodymium in a $\text{Na}^+\text{-Cl}^-\text{-CO}_3^{2-}\text{-HCO}_3^-$ solution system [11], shows that there is a relationship between the solubility of rare earth in a carbonate solution and the concentration of the NaCl salt as an impurity, and the dissolved amount of rare earth increases with increasing concentration of NaCl in the solution. High concentration of NaCl results in high ionic strength of the solution. In addition, according to research data on rare earth adsorption in a water-bearing sand layer [12], at higher ionic strength of the solution, the more significant was the rare earth adsorption in the sand layer. In other words, a greater amount of rare earth loss was caused by dissolution. Thus, when the concentration of NH_4^+ in the solution increased, this resulted in a greater amount of dissolved rare earths, as observed by Vasconcellos [10], which can be attributed to the influence of the ionic strength of the solution [13].

Nowadays, a number of techniques have been developed for the separation of rare earths, such as solvent extraction [14], ion exchange, membrane separation and ionic liquids [15], as well as other methods. Among them, the most widely used is the traditional solvent extraction technique. The other methods are less used because of high cost. The core component of solvent extraction is the extractant. Currently, a number of high-performance extractants have been developed [16], but toxicity and loss of extractants are always the key weaknesses limiting the development of the technology. In addition, due to the increasingly stringent requirements of environmental protection, the high salt wastewater generated during the separation of rare earths remains a problem [17], and is also a bottleneck in the solvent extraction separation process [18]. For the healthy development of the rare earth industry, it is necessary and urgent to develop a new type of highly efficient and environmentally friendly separation technology.

A good and feasible green method to separate rare earths is by using the metastable state of the carbonate solution which dissolves them. In our previous study [19], a series of experiments on metastable states was carried out by choosing neodymium as an example of rare earth elements. Our results indicated that neodymium dissolved in a sodium carbonate solution exhibited some metastable properties. Among them, the most important one was that there is a limit to the dissolution of neodymium in a certain concentration of sodium carbonate solution, after which there is instantaneous saturated solubility. When the dissolved neodymium in the solution does not exceed its solubility, it is stable in the solution for a period (metastable period) without precipitating neodymium carbonate. Our previous study was not very comprehensive and limited by the length of the paper, so a follow-up study of metastable solution-induced precipitation was not carried out.

Now, combined with the idea of the solid-liquid separation of rare earths, we are continuing to consider the potential value of the metastable state. Rare earths are dissolved and enriched in the metastable period and precipitated and separated after exceeding this period. No other impurities are introduced in this process. In addition, the carbonate solution can be recycled. Therefore, this may be a potential method for green separation of rare earths. Hence, how to manually control the metastable state and the precipitation of rare earth carbonate is the core content of the present study.

In this study, the artificial control of metastable states is discussed in detail. Neodymium was chosen as a representative of rare earth elements. The effect of changing the solution environment, such as ion concentration, on the metastable state was studied, and the effective conditions for maintaining and destroying the metastable state were discovered.

2. Experiment

2.1. Raw Materials and Equipment

The rare earth material used in the experiment was a $10 \text{ g}\cdot\text{L}^{-1}$ dilute NdCl_3 solution obtained by diluting high purity NdCl_3 solution with deionized water. The high purity NdCl_3 solution was purchased from the rare earth smelting & separating plant in Longnan, Jiangxi Province, and its distribution is shown in Table 1. Solutions of Na_2CO_3 , $\text{Na}_2\text{CO}_3/\text{NaCl}$ with different concentration gradients and dilute hydrochloric acid for acidification were obtained by dissolving AR-grade Na_2CO_3 , solid NaCl and HCl solution with deionized water.

Table 1. Content of the high purity solution of NdCl_3 .

Concentration of Nd^{3+} ($\text{mol}\cdot\text{L}^{-1}$)		Concentration of H^+ ($\text{mol}\cdot\text{L}^{-1}$)		Specific Gravity ($\text{g}\cdot\text{mL}^{-1}$)		
1.3568		<0.10		1.326		
Non-rare earths impurities ($\mu\text{g}\cdot\text{mL}^{-1}$)						
Fe_2O_3 <0.50		SiO_2 2.49		CaO 7.3		
Rare Earth Impurities/REO ($\mu\text{g}\cdot\text{mL}^{-1}$)						
La_2O_3 <100	CeO_2 <100	Pr_6O_{11} 500	Sm_2O_3 <100	Eu_2O_3 <100	Gd_2O_3 <100	Tb_2O_3 <100
Dy_2O_3 <100	Ho_2O_3 <100	Er_2O_3 <100	Tm_2O_3 <100	Yb_2O_3 <100	Lu_2O_3 <100	Y_2O_3 <100

An experiment in which CO_2 gas was used to induce precipitation of a metastable state solution was carried out by using an autoclave with a CO_2 high-pressure cylinder, as shown in Figure 1. Other equipment used in experiments is shown in Table 2.

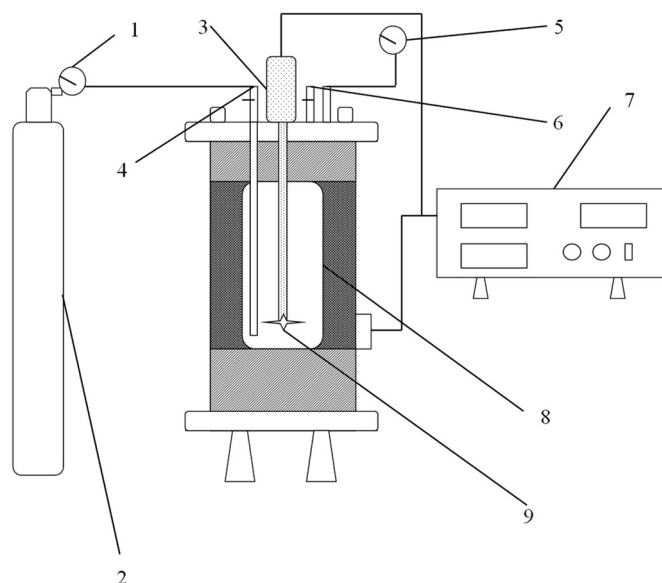


Figure 1. Schematic diagram of autoclave ventilation experiment: 1— CO_2 pressure reducing valve; 2—high pressure cylinder; 3—rotating motor; 4—air inlet; 5—safety valve; 6—air outlet; 7—controller; 8—polytetrafluoroethylene tank; 9—agitator.

Table 2. Information of equipment.

Equipment	Model	Manufacturers
High-speed centrifuge	TGL16MS	Yancheng Anxin Experimental Instrument Co., Ltd. (Yancheng, China)
Computing server	IBM System X3850 X5	International Business Machines Corporation (Armonk, NY, USA)
UV-Visible Spectrophotometer (UV-vis)	UV-5500PC	Shanghai yoke instrument Co., Ltd. (Shanghai, China)
Fourier transform infrared spectrometer (FTIR)	ALPHA	Bruker Corporation (Billerica, MA, USA)
inductively coupled plasma-optical emission spectroscopy (ICP-OES)	ULTIMA2	HORIBA Jobin Yvon (Newark, NJ, USA)
Kang's oscillator	KS	Changzhou Putian Instrument Manufacturing Company (Changzhou, China)

2.2. Maintenance and Mechanism of Metastable State of the Neodymium Dissolved in Na_2CO_3 Solution

2.2.1. Maintaining Metastable State by NaCl

Following on from our previous research [19], the effect of additional NaCl on the maintenance of the metastable state of a solution of dissolved Nd^{3+} was investigated. The neodymium concentration in $2 \text{ mol}\cdot\text{L}^{-1}$ Na_2CO_3 solution was controlled at $2.621 \text{ g}\cdot\text{L}^{-1}$. The ionic strength of the solution was controlled by adding NaCl to Na_2CO_3 solution to create a mixed electrolyte NaCl/ Na_2CO_3 solution. The concentration of the additional NaCl ranged from 0 to $0.5 \text{ mol}\cdot\text{L}^{-1}$. During the experiment, the volume of the Na_2CO_3 (or mixed electrolyte NaCl/ Na_2CO_3) solution was fixed at 25 mL, and the NdCl_3 solution was added to it drop by drop with oscillation. The time was set from 0 to 480 min. When the experiment finished, the solution containing precipitates was further centrifuged at 6000 rpm for 5 min. After that, the obtained supernatant was split into two parts; one was selected as aqueous sample for the further testing, and the another was completely acidulated by using dilute hydrochloric acid, after which complexometric titration was used to determine the concentration of Nd^{3+} .

2.2.2. Effect of NaCl on Neodymium Coordination and Solid Phase Precipitates

The metastable state solution in each representative stationary period was scanned by ultraviolet-visible light (UV-vis) full-wavelength scanning. In order to provide an experimental comparison, a blank solution (Na_2CO_3 and NdCl_3 solution only addition with water) was also scanned by UV-vis full wavelength. The precipitates were collected as solid samples and detected by Fourier transform infrared spectroscopy (FTIR). Because drying could cause the sample to decompose [20], producing errors in the results, the samples were all stored in deionized water. Before determination, the water was filtered, the samples dried with filter paper, and the analysis carried out immediately.

2.2.3. Mechanism of Maintaining the Metastable State by NaCl

In order to find the maintenance mechanism of the additional NaCl on the metastable state, a molecular dynamics (MD) calculation was carried out using Materials Studio 8.0 [21] software. The solution model was established by using an Amorphous Cell module, and the model was geometry optimized using a Forcite module. Finally, MD calculation and radial distribution function (RDF) analysis [22] were carried out to reveal the relationship between the RDF and the coordination number of each component in the solution. The average coordination number of each component was calculated by Equation (1).

$$N(L) = \int_0^L g(r) \rho 4\pi r^2 dr \quad (1)$$

where $N(L)$ refers to the number of coordination atoms(molecules) in the 0– L spherical shell around the target atom, ρ refers to the number density of coordination atoms (molecules), where the value is the ratio of the number of atoms (molecules) to the volume of space, $g(r)$ refers to the RDF value, and indicates the probability of the occurrence of coordination atoms(molecules) within a certain distance, and r refers to the cutoff radius.

2.3. Induced Precipitation of Neodymium Carbonates in Metastable State Solution

The precipitation process of neodymium carbonates by introducing CO_2 gas into the metastable state solution was studied. The procedure of the dissolution of Nd^{3+} in the solution was as previously described. Further, the dissolved Nd^{3+} solution was transferred to an autoclave for introducing CO_2 gas. The solution contained a large amount of halogen Cl^- , so a corrosion-resistant polytetrafluoroethylene tank was selected as the inner tank of the autoclave. During the experiment, the input pressure of CO_2 was uniformly controlled at 0.2 Mpa. The time was set from 0–60 min. When the set time was reached, the solution containing precipitate was centrifuged at $6000 \text{ r}\cdot\text{min}^{-1}$ for 5 min, then the supernatant obtained after centrifugation was split in two parts. One was acidified, and the concentration of neodymium in the supernatant was determined by inductively coupled plasma emission spectrometer (ICP-OES). The other was analyzed by CO_3^{2-} and HCO_3^- acid-base titration to determine the concentration of CO_3^{2-} and HCO_3^- .

3. Results and Discussion

3.1. Maintenance and Mechanism of the Metastable State of Neodymium Dissolved in Na_2CO_3 Solution

3.1.1. Maintaining Metastable State by NaCl

The metastable period of the solution with the addition of NaCl was greater than that of the solution without NaCl due to neodymium being dissolved stably in solution for a longer time. As shown in Figure 2a, the metastable period was sustained only for about 120 min without the addition of NaCl. However, the metastable period reached 240 min when the concentration of the additional NaCl was $0.2 \text{ mol}\cdot\text{L}^{-1}$. Moreover, the amount of dissolved neodymium in the solution reached $2.578 \text{ g}\cdot\text{L}^{-1}$, which was only 1.64% lower than the initial amount of $2.621 \text{ g}\cdot\text{L}^{-1}$. Surprisingly, when the additional concentration of sodium chloride in the solution reached $0.5 \text{ mol}\cdot\text{L}^{-1}$, the metastable period was extended to 480 min, i.e., twice as long as before.

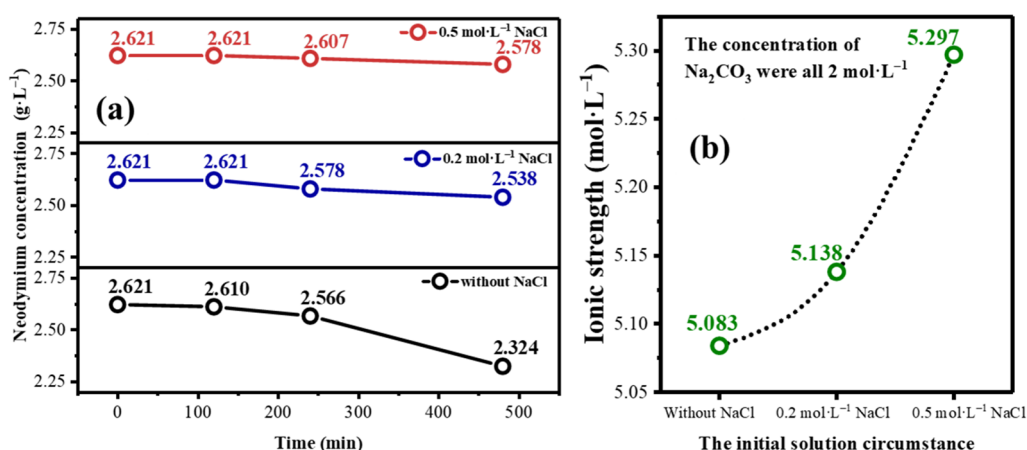


Figure 2. The effect of the concentration of the additional NaCl in (a) and Ionic strength of solution in (b).

The molar concentration in the above solution was converted into mass molar concentration according to Equation (2). Then, the ionic strength of each solution was calculated

by using Equation (3). The results are shown in Figure 2b which shows that the addition of NaCl effectively improved the ionic strength of the solution.

$$C = bB \cdot \rho \quad (2)$$

$$I = \frac{1}{2} \sum C_i b B_i^2 \quad (3)$$

bB refers to the molar concentration, ρ refers to the density of the solution, and I refers to the ionic strength of the solution.

In the case of the equivalent concentration of Na_2CO_3 , the addition of NaCl resulted in neodymium dissolving stably in Na_2CO_3 solution for a longer time. The higher the concentration of NaCl in solution, and the stronger the ionic strength, resulting in a longer metastable period of the solution. Hence, the additional NaCl maintained the metastable state effectively.

3.1.2. Effect of NaCl on Neodymium Coordination and Solid Phase Precipitates

To confirm whether the coordination reaction between Nd^{3+} and CO_3^{2-} still occurred in the mixed electrolyte solution of $\text{NaCl}/\text{Na}_2\text{CO}_3$, the aqueous samples in each period of the above experiments were collected and scanned by UV-vis with full wavelength. As shown in Figure 3, the characteristic peak of neodymium was not found in the UV-vis spectra of the sample of the blank $\text{NaCl}/\text{Na}_2\text{CO}_3$ mixed electrolyte solution with only added water. Characteristic peaks of neodymium at the 340–370 nm and 500–620 nm wavebands [23] were observed in the spectra of the blank NdCl_3 solution with added water only.

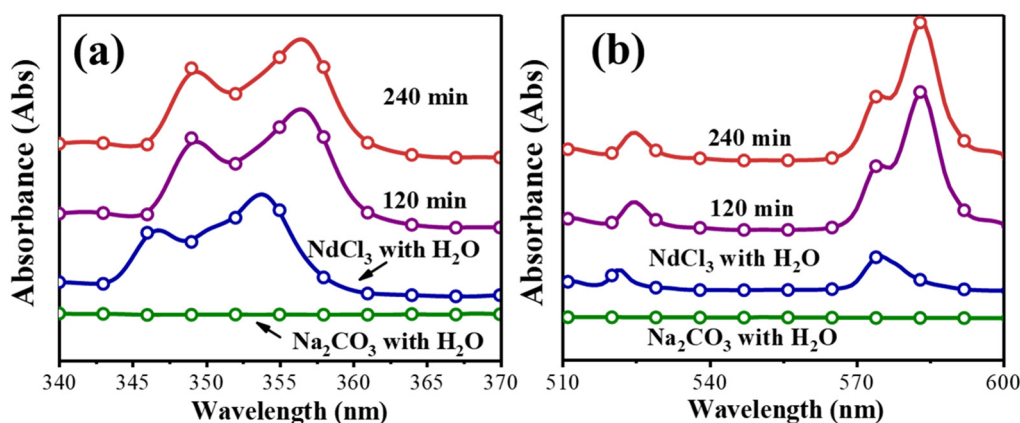


Figure 3. UV-vis spectrum of $\text{NdCl}_3/\text{Na}_2\text{CO}_3$ solution with the addition of 0.5M NaCl, wavelength in 340 to 370 nm in (a), and 510 to 600 nm in (b).

As shown in Figure 3, characteristic peaks of neodymium were obtained at 349 and 357 nm wavelengths in the spectra of the $\text{NaCl}/\text{Na}_2\text{CO}_3$ mixed electrolyte solution with dissolved neodymium. Compared with the blank neodymium solution spectrum, it is worth noting that the characteristic peaks of neodymium obtained from the $\text{NaCl}/\text{Na}_2\text{CO}_3$ solutions with dissolved neodymium were slightly red-shifted from the initial 347 and 354 nm wavelengths due to the high alkalinity of the $\text{NaCl}/\text{Na}_2\text{CO}_3$ mixed electrolyte solution.

There were also neodymium characteristic peaks at 524 and 575 nm wavelengths in the UV-vis spectrum of the neodymium-dissolving solution, as in our previously results [19]. In addition, a new peak with higher intensity was observed at 583 nm. This indicates that neodymium could still coordinate with CO_3^{2-} in the Na_2CO_3 solution with the addition of NaCl. The precipitate sample generated from the solution after 480 min was collected and analyzed by FTIR. The results shown in Figure 4.

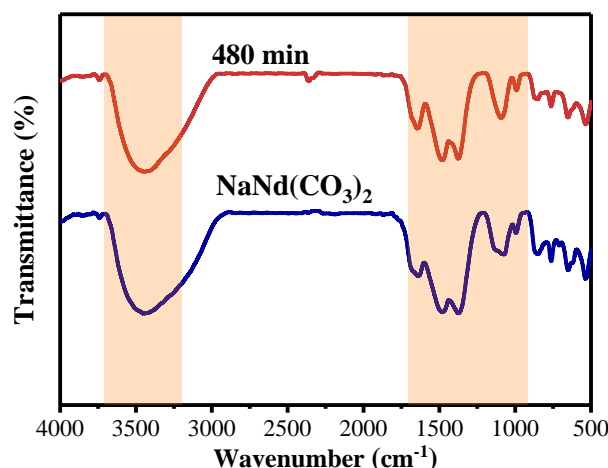


Figure 4. FTIR pattern of the neodymium precipitate, red line refers to the precipitate obtained in the presence of 0.5 mol NaCl, and blue line refers to the Comparison sample.

Figure 4 shows that the characteristic infrared peak position of the precipitate generated from the NaCl/Na₂CO₃ solution with dissolved neodymium was consistent with that of the blank sample NaNd(CO₃)₂ solid phase. This was consistent with results reported in previous studies [11,24]. These reports and our results confirm that in the presence of additional NaCl in a highly concentrated CO₃²⁻ solution, the insoluble rare earth existed only in the form of an NaNd(CO₃)₂ double salt, while Nd₂(CO₃)₃ was almost non-existent.

3.1.3. Mechanism of Maintaining the Metastable State by NaCl

In order to investigate the mechanism of the maintenance of the metastable state by the additional NaCl, molecular dynamic (MD) calculations were carried out. The construction and optimization of the solution components were consistent with our previous study [19]. The model of the solution with the addition of 0.5 mol·L⁻¹ NaCl (with the better metastable condition), and the corresponding blank solution (Na₂CO₃/NaCl solution with the only additional water) was also established by using the Amorphous Cell module. After that, geometry optimization and the MD calculation were carried out. The components in the model and calculation parameters are shown in Table 3. The energy changed during the geometry optimization process is presented in Figure 5a.

Table 3. Modeling parameters of the solutions.

Components	The Metastable State Solution		Corresponding Blank Solution	
	$\rho: 1.164 \text{ g}\cdot\text{L}^{-1}$		$\rho: 1.148 \text{ g}\cdot\text{L}^{-1}$	
	Number	Mass Fraction (%)	Number	Mass Fraction (%)
H ₂ O	10,590	84.7	10,590	85.0
Na ⁺	630	6.4	630	6.5
CO ₃ ²⁻	280	7.5	280	7.5
Nd ³⁺	3	0.2	0	0.0
Cl ⁻	79	1.2	70	1.1

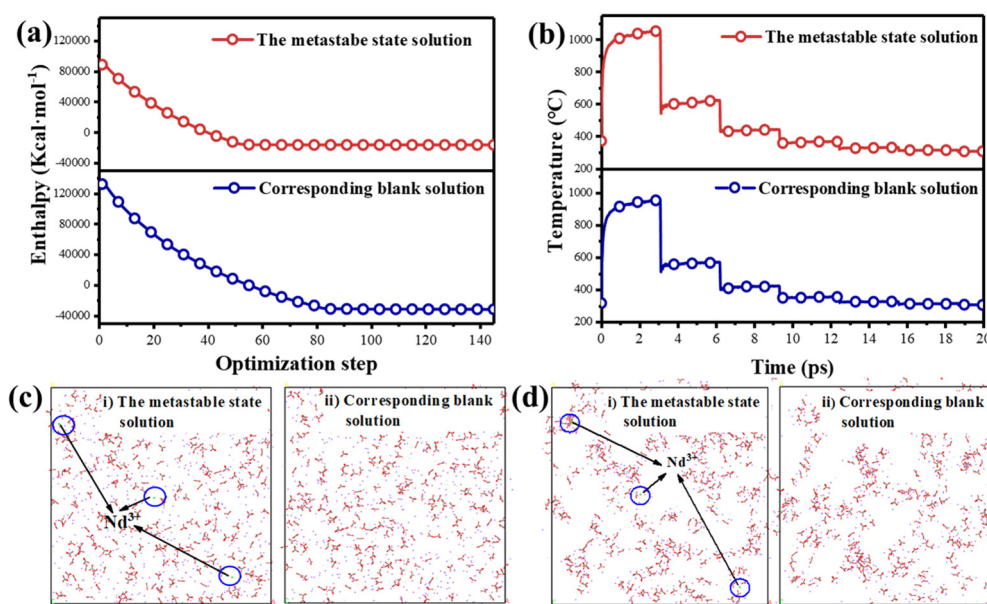


Figure 5. Geometry optimization process of the solution model (a). Temperature change during the MD calculation in (b). Geometry optimization and after MD calculation of the solution model (c,d). In the figures, (i) refers to the metastable state solution and (ii) is the corresponding blank solution.

As shown in Figure 5a, the overall energy decreased gradually with increase in the number of optimization steps without large energy disturbances. At the end of optimization, the energy tended to be relatively minimized and achieved convergence. Change of the temperature is presented in Figure 5b, which shows that the temperature of the models decreased gradually with the increase of simulation time. At the end of the calculation, it was stable at about $298\text{ K} \pm 10\%$ and there was no significant disturbance. This result is very reliable. The optimized models are presented in Figure 5c, which shows that after the geometry optimization step, the Na^+ , CO_3^{2-} , Nd^{3+} , Cl^- ions in each solution model were randomly and uniformly distributed in the model box, and no agglomeration existed.

The models after the MD calculation are presented in Figure 5d, which shows that the solution was generally homogeneous. However, in the local region, the components of the solution model had different degrees of agglomeration due to the interaction between ions (or molecules). Among them, the CO_3^{2-} distribution exhibited local agglomeration. A large number of Na^+ ions were distributed around the CO_3^{2-} . This can be attributed to the incomplete dissociation of Na^+ and CO_3^{2-} at the high concentration of the $\text{NaCl}/\text{Na}_2\text{CO}_3$ mixed electrolyte solution. We speculate that the concentration of carbonate that could move freely (called free CO_3^{2-}) in the solution was limited and at a low level.

Moreover, Nd^{3+} was also almost surrounded by CO_3^{2-} in that Nd^{3+} was coordinated with about three CO_3^{2-} . This shows that Nd^{3+} can coordinate with carbonate despite the addition of NaCl to Na_2CO_3 solution. In addition, all kinds of complex ions in the form of $\text{Nd}_n(\text{CO}_3)_m^{3n-2m}$ ($m \geq 2$) existed, but in different proportions. As shown in Figure 6a, there was a specific Cl^- ion around some Nd^{3+} ions, indicating that, unlike in previous studies, Cl^- might also coordinate with Nd^{3+} . Previous studies of steady-state dissolution of rare earths in CO_3^{2-} solution [11,24], showed that the coordination between Cl^- and Nd^{3+} could almost be ignored under the condition of steady-state solution equilibrium because of weak Cl^- coordination ability, which does not agree with our study. The difference could be ascribed to the difference between metastable and steady states. Besides, it is reasonable to speculate that Cl^- occupied the coordination layer of Nd^{3+} , delaying the formation of carbonate precipitation. Therefore, the addition of NaCl maintained the metastable state.

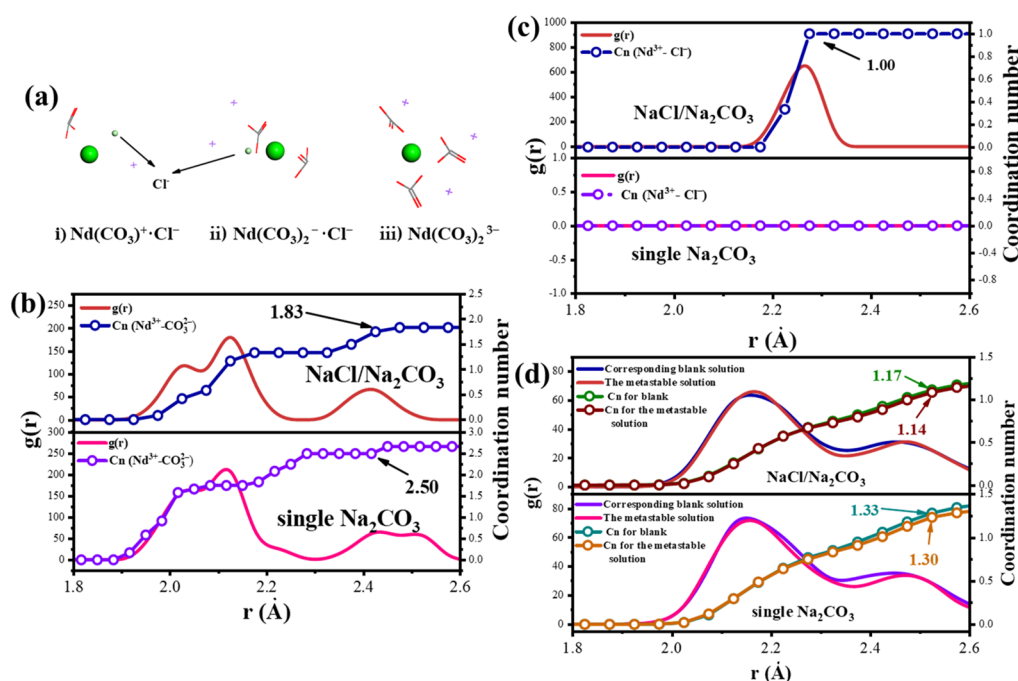


Figure 6. Coordination between Nd^{3+} , Cl^- & CO_3^{2-} (a). RDF of the ion pairs $\text{Nd}^{3+}\text{-CO}_3^{2-}$, $\text{Nd}^{3+}\text{-Cl}^-$ & $\text{Na}^+\text{-CO}_3^{2-}$ and their coordination number (b–d), respectively.

In order to further quantify the interaction from the microscopic level, the main ion pairs of $\text{Nd}^{3+}\text{-CO}_3^{2-}$, $\text{Na}^+\text{-CO}_3^{2-}$ and $\text{Nd}^{3+}\text{-Cl}^-$ in the solution were analyzed by radial distribution function (RDF), and their coordination numbers were calculated. Figure 6b shows that the RDF peak position of Nd^{3+} and CO_3^{2-} in the $\text{NaCl}/\text{Na}_2\text{CO}_3$ mixed electrolyte solution was almost the same as that in the single Na_2CO_3 solution in the chemical bond range ($r < 2.6 \text{ \AA}$) [25]. This directly proves that Nd^{3+} can coordinate with CO_3^{2-} even in the presence of NaCl . At the same time, the RDF peak intensity of $\text{Nd}^{3+}\text{-CO}_3^{2-}$ in the presence of NaCl was slightly lower than that in the single Na_2CO_3 solution. The difference of RDF peak intensity indicated that the additional NaCl had an influence on the interaction between Nd^{3+} and CO_3^{2-} . From the point of view of coordination number, with the presence of the additional NaCl the average coordination number around Nd^{3+} was about 1.83 CO_3^{2-} , which was lower than the average coordination number of 2.50 in the single Na_2CO_3 solution. The reason for the decrease of coordination number may be that part of Cl^- occupied the coordination layer of Nd^{3+} in the metastable period, causing the decrease in the average coordination number between Nd^{3+} and CO_3^{2-} . This is consistent with Figure 6a.

To quantitatively explain the coordination between Nd^{3+} and Cl^- in the mixed electrolyte, the RDF and the coordination number were further analyzed and calculated. Figure 6c shows that the RDF peak at 2.275 \AA within the range of chemical bond ($< 2.6 \text{ \AA}$) was clearly observed from the spectrum of the $\text{Nd}^{3+}\text{-Cl}^-$ ion pair in the mixed electrolyte solution of $\text{NaCl}/\text{Na}_2\text{CO}_3$. One Nd^{3+} was coordinated with about one Cl^- . In contrast to the single Na_2CO_3 solution, there was insignificant evidence of an interaction existing between Cl^- and Nd^{3+} . Hence, it was proved that Cl^- could coordinate with Nd^{3+} in the presence of NaCl during the metastable period.

It is worth noting that the RDF peak position of $\text{Nd}^{3+}\text{-CO}_3^{2-}$ was earlier than that of $\text{Nd}^{3+}\text{-Cl}^-$. The result indicates that CO_3^{2-} tends to occupy the coordination layer of Nd^{3+} and reacted with it first, then Cl^- entered the coordination layer of Nd^{3+} , although, previous studies [11,24] showed that in an environment of high concentration of CO_3^{2-} solution, Cl^- did not coordinate with Nd^{3+} in a steady state. However, our result does not conflict with these previous studies because of the difference between metastable and steady states. In addition, when the placement time exceeded the metastable period, the precipitate

was still consistent with that obtained in the steady state. Therefore, there is sufficient reason to speculate that in the metastable state, Cl^- participated in the coordination reaction and temporarily occupied the coordination layer of Nd^{3+} , and then was re-released into the solution with the passage of time. When the metastable period ended, the Cl^- in the coordination layer of Nd^{3+} had been exhausted. A diagram of Nd^{3+} , Cl^- and CO_3^{2-} coordination in the metastable state is shown in Figure 7.

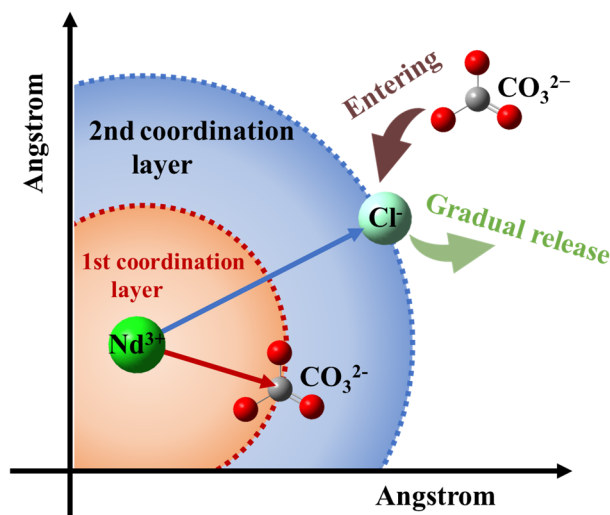


Figure 7. Coordination process of Nd^{3+} in the $\text{NaCl}/\text{Na}_2\text{CO}_3$ mixed electrolyte solution.

The concentration of free CO_3^{2-} in solution was another key factor affecting the existence of metastable states. To explore the interaction between Na^+ and CO_3^{2-} in the solution in the presence of additional NaCl , the RDF of the $\text{Na}^+ - \text{CO}_3^{2-}$ ion pair and its average coordination number were also analyzed and calculated. The results in Figure 6d show that there was interaction between Na^+ and CO_3^{2-} in the mixed electrolyte solution, and the position of the RDF peak was basically the same as that in single Na_2CO_3 solution. The average coordination number was about 1.14 CO_3^{2-} around a Na^+ ion in the solution with additional NaCl , which was not much different from the corresponding blank solution number of 1.17. However, the value was lower than the value of 1.30 in a single Na_2CO_3 solution.

The existence of this difference does not mean that the degree of dissociation of $\text{Na}^+ - \text{CO}_3^{2-}$ ion pairs in the mixed electrolyte solution was higher because of the introduction of Na^+ via the addition of NaCl . The introduced Na^+ would also tend to interact with CO_3^{2-} , reducing the average coordination number. In this regard, the conversion calculation of the number of Na^+ ions around the CO_3^{2-} is a better illustration of the problem, as listed in Table 4.

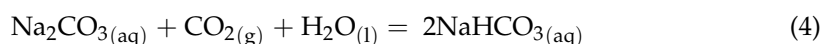
Table 4. Distribution of Na^+ around CO_3^{2-} in the solution.

r (Å)	Average Coordination Number (Cn)	
	NaCl/ Na_2CO_3 Mixed Electrolyte Solution	Single Na_2CO_3 Solution
2.225	1.29	1.28
2.275	1.51	1.50
2.325	1.64	1.67
2.375	1.79	1.82
2.425	1.99	2.02
2.475	2.24	2.26
2.525	2.44	2.46
2.575	2.57	2.57
2.625	2.63	2.63

Table 4 shows that the distribution of Na^+ around CO_3^{2-} in mixed electrolyte and single Na_2CO_3 solutions was the same at a cutoff distance of 2.575 Å (within chemical bond range), which was 2.57 Na^+ around CO_3^{2-} . The total number of Na^+ was 630 in the mixed electrolyte, higher than that of 580 in a single Na_2CO_3 solution, due to the existence of additional NaCl . Even so, the distribution of Na^+ around CO_3^{2-} was almost the same. This means that the dissociation degree of the Na^+ - CO_3^{2-} ion pairs with the additional NaCl should be much lower than that in the single Na_2CO_3 solution. Therefore, the additional NaCl could also affect the interaction of Na^+ - CO_3^{2-} ion pairs, further reducing the concentration of free CO_3^{2-} . Thus, the delayed the formation of neodymium carbonates was delayed and the metastable period was extended.

3.2. Induced Precipitation of Neodymium Carbonates in Metastable State Solution

In theory, if the system dominated by CO_3^{2-} in the solution could be rapidly transformed into the coexistence of HCO_3^- and CO_3^{2-} , a rapid destruction of metastable state could be achieved and most of the dissolved neodymium could be separated from the solution via a self-precipitation. Theoretically, introduction of acidic CO_2 gas into the solution, as shown in Equation (4), would neutralize the original alkaline Na_2CO_3 solution so that the induction of neodymium carbonate from the metastable solution might be more quickly achieved.



The specific experimental results in Figure 8a show that the metastable state was rapidly terminated after the introduction of CO_2 gas. The concentration of dissolved Nd^{3+} in the solution fell rapidly, and neodymium carbonate precipitate were generated and separated from the solution. After gassing with CO_2 for only 5 min, the Nd^{3+} concentration in the solution decreased from 2.621 to 1.793 $\text{g}\cdot\text{L}^{-1}$, and the precipitation rate reached 31.60%. When the ventilation time was extended to 30 min, only 0.239 $\text{g}\cdot\text{L}^{-1}$ was left in the solution, and the precipitation rate of Nd^{3+} reached 90.87%. When the ventilation time reached 60 min, the neodymium concentration in the solution further decreased from 0.239 $\text{g}\cdot\text{L}^{-1}$ at 30 min to 0.138 $\text{g}\cdot\text{L}^{-1}$, and the precipitation rate slowly increased from 90.78% to almost 95%. The results indicate that Nd^{3+} in the solution entered the insoluble solid phase and was separated from the solution via self-precipitation.

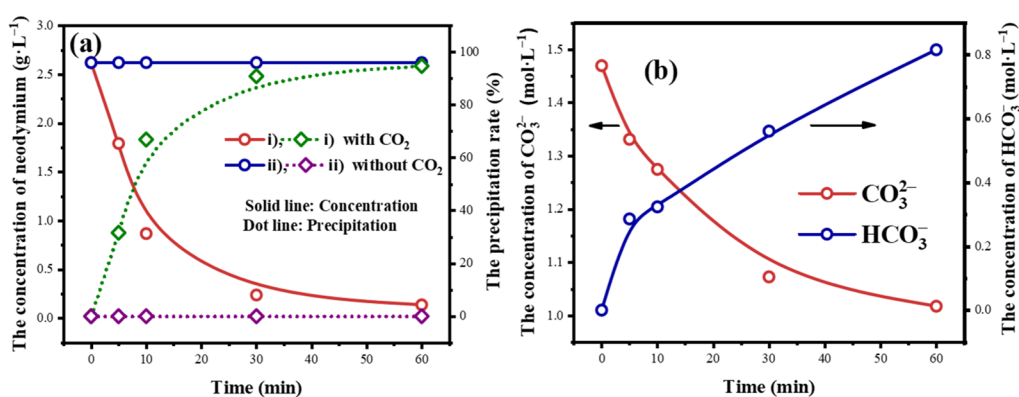


Figure 8. The concentration of dissolved Nd^{3+} in the solution and the precipitation rate with the ventilation time of CO_2 (a), and the concentration of CO_3^{2-} / HCO_3^- with the ventilation time of CO_2 (b).

Acid-base titration analysis was carried out to determine the concentration of CO_3^{2-} and HCO_3^- in the solution after CO_2 was injected. Figure 8b shows that the concentration of CO_3^{2-} in the solution decreased with increasing CO_2 introduction time. The concentration of HCO_3^- showed an upward trend during the introduction of CO_2 , and the system gradually changed from a single CO_3^{2-} -dominated to a CO_3^{2-} and HCO_3^- -dominated system.

When the CO₂ introduction time reached 5 min, the concentration of HCO₃[−] in the solution approached 0.286 mol·L^{−1} and the corresponding concentration of CO₃^{2−} was 1.331 mol·L^{−1}, which was much lower than the initial value of 2 mol·L^{−1}. After 60 min, the concentration of HCO₃[−] in the solution increased than several times and reached about 0.816 mol·L^{−1}. Besides, the corresponding concentration of CO₃^{2−} was reduced to 1.018 mol·L^{−1}, and the solution system could no longer be considered to be dominated by single CO₃^{2−}, but both CO₃^{2−} and HCO₃[−]. The reason was that the solution of NaCl/Na₂CO₃ mixed electrolyte with higher basicity spontaneously absorbed acidic CO₂ gas, resulting in the conversion of CO₃^{2−} to HCO₃[−] in a short time.

After introducing CO₂, the concentration of CO₃^{2−} in the solution decreased, but the solution volume was almost unchanged. In other words, it was equivalent to diluting the solution. It is well known that ion pairs dissociate more completely in dilute solution. Thus, there is no doubt that the concentration of free CO₃^{2−} in the solution was increased, and it is important that CO₂ could induce the precipitation of neodymium carbonate in the metastable state solution. In addition, the concentration of CO₃^{2−} decreased as CO₂ introduction time and the precipitation rate of neodymium carbonate increased. Therefore, the introduction of carbon dioxide into metastable solutions is a new potential method for the separation of rare earths. This is because carbon dioxide is nonpolluting and does not introduce other ion impurities as with the use of precipitants (e.g., ammonium carbonate, which is commonly used in industry, introduces ammonium ions). In addition, the separation is achieved by the rapid production of rare earth precipitation in a short time after its entry into the solution.

4. Conclusions

We chose neodymium as an example of a rare earth element and studied the maintenance of the metamorphic state of Na₂CO₃ solution with dissolved Nd³⁺. The results show that the metastable state can be successfully prolonged by adding sodium chloride. In addition, the introduction of carbon dioxide is an effective way to terminate the metastable state and generate neodymium carbonate.

The main conclusions are as follows. (1) The higher the additional NaCl concentration, the longer the metastable period, because the additional NaCl affects the interaction of Na⁺-CO₃^{2−}-ion pairs and influences the concentration of free CO₃^{2−} in the solution. (2) The Cl[−] introduced by the high concentration of NaCl can occupy the coordination layer of Nd³⁺ temporarily and delay the formation of rare earth carbonate precipitation. (3) After introduction of CO₂ gas, the existing environment of the solution directly changes in a short time from a single CO₃^{2−}-dominated system to a predominantly CO₃^{2−} and HCO₃[−]-dominated system. As a result, the metamorphic state of the solution is quickly terminated and the precipitation of Nd carbonate is advanced.

Author Contributions: Conceptualization, K.L.; data curation, X.Z.; formal analysis, Y.M.; funding acquisition, Y.Y.; investigation, K.L.; methodology, K.L.; project administration, Y.Y.; validation, F.N.; visualization, K.L.; writing—original draft, K.L.; writing—review & editing, L.W. and D.L. All authors have read and agreed to the published version of the manuscript.

Funding: This research was funded by National Natural Science Foundation of China, grant number 51774155, and The APC was funded by 51774155.

Data Availability Statement: Not Applicable.

Acknowledgments: The authors gratefully acknowledge the financial supports of the Program of National Natural Science Foundation of China (51774155).

Conflicts of Interest: The authors declare no conflict of interest.

References

1. Takagi, K.; Hirayama, Y.; Okada, S.; Yamaguchi, W.; Ozaki, K. Novel powder processing technologies for production of rare-earth permanent magnets. *Sci. Technol. Adv. Mater.* **2021**, *22*, 150–159. [[CrossRef](#)] [[PubMed](#)]

2. Prokofev, P.A.; Kolchugina, N.B.; Skotnicova, K.; Burkhanov, G.S.; Kursa, M.; Zheleznyi, M.V.; Dormidontov, N.A.; Cegan, T.; Bakulina, A.S.; Koshkidko, Y.S.; et al. Blending Powder Process for Recycling Sintered Nd-Fe-B Magnets. *Materials* **2020**, *13*, 3049. [[CrossRef](#)] [[PubMed](#)]
3. Nelson, J.J.M.; Schelter, E.J. Sustainable Inorganic Chemistry: Metal Separations for Recycling. *Inorg. Chem.* **2019**, *58*, 979–990. [[CrossRef](#)] [[PubMed](#)]
4. Lixandru, A.; Venkatesan, P.; Jönsson, C.; Poenaru, I.; Hall, B.; Yang, Y.; Walton, A.; Güth, K.; Gauß, R.; Gutfleisch, O. Identification and recovery of rare-earth permanent magnets from waste electrical and electronic equipment. *Waste Manag.* **2017**, *68*, 482–489. [[CrossRef](#)] [[PubMed](#)]
5. Kuz'Min, M.D.; Skokov, K.; Jian, H.; Radulov, I.; Gutfleisch, O. Towards high-performance permanent magnets without rare earths. *J. Phys. Condens. Matter* **2014**, *26*, 64205. [[CrossRef](#)] [[PubMed](#)]
6. Bingqian, W. *Rare Earth Metallurgy*; Central South University of Technology Press: Changsha, China, 1997.
7. Firsching, F.H.; Mohammadzadei, J. Solubility products of the rare-earth carbonates. *J. Chem. Eng. Data* **1986**, *31*, 40–42. [[CrossRef](#)]
8. Taketatsu, T. The solubilities and anion-exchange behavior of rare earth elements in potassium carbonate solutions. *Anal. Chim. Acta* **1965**, *32*, 40–45. [[CrossRef](#)]
9. Taketatsu, T. The Dissolution and Anion Exchange Behavior of Rare Earth and Other Metallic Elements in Potassium Bicarbonate, Potassium Carbonate and Ammonium Carbonate Solutions. *Bull. Chem. Soc. Jpn.* **1963**, *36*, 549–553. [[CrossRef](#)]
10. de Vasconcellos, M.E.; da Rocha, S.; Pedreira, W.; Queiroz, C.A.D.S.; Abrão, A. Solubility behavior of rare earths with ammonium carbonate and ammonium carbonate plus ammonium hydroxide: Precipitation of their peroxycarbonates. *J. Alloy. Compd.* **2008**, *451*, 426–428. [[CrossRef](#)]
11. Rao, L.; Rai, D.; Felmy, A.R.; Novak, C.F. Solubility of $\text{NaNd}(\text{CO}_3)_2 \cdot 6\text{H}_2\text{O}$ (c) in Mixed Electrolyte ($\text{Na}-\text{Cl}-\text{CO}_3-\text{HCO}_3$) and Synthetic Brine Solutions. In *Actinide Speciation in High Ionic Strength Media*; Springer: Berlin/Heidelberg, Germany, 1999; pp. 153–169.
12. Tang, J.; Johannesson, K.H. Rare earth elements adsorption onto Carrizo sand: Influence of strong solution complexation. *Chem. Geol.* **2010**, *279*, 120–133. [[CrossRef](#)]
13. Thakur, P.; Xiong, Y.; Borkowski, M. An improved thermodynamic model for the complexation of trivalent actinides and lanthanide with oxalic acid valid to high ionic strength. *Chem. Geol.* **2015**, *413*, 7–17. [[CrossRef](#)]
14. Jing, Y.; Chen, J.; Chen, L.; Su, W.; Liu, Y.; Li, D. Extraction Behaviors of Heavy Rare Earths with Organophosphoric Extractants: The Contribution of Extractant Dimer Dissociation, Acid Ionization, and Complexation. A Quantum Chemistry Study. *J. Phys. Chem. A* **2017**, *121*, 2531–2543. [[CrossRef](#)] [[PubMed](#)]
15. Pavón, S.; Fortuny, A.; Coll, M.; Sastre, A.M. Rare earths separation from fluorescent lamp wastes using ionic liquids as extractant agents. *Waste Manag.* **2018**, *82*, 241–248. [[CrossRef](#)] [[PubMed](#)]
16. Qiu, L.; Pan, Y.; Zhang, W.; Gong, A. Application of a functionalized ionic liquid extractant tributylmethylammonium dibutyldiglycolamate ([A336][BDGA]) in light rare earth extraction and separation. *PLoS ONE* **2018**, *13*, e0201405. [[CrossRef](#)]
17. Sun, P.; Huang, K.; Liu, H. The nature of salt effect in enhancing the extraction of rare earths by non-functional ionic liquids: Synergism of salt anion complexation and Hofmeister bias. *J. Colloid Interface Sci.* **2019**, *539*, 214–222. [[CrossRef](#)]
18. Li, C.; Zhuang, Z.; Huang, F.; Wu, Z.; Hong, Y.; Lin, Z. Recycling Rare Earth Elements from Industrial Wastewater with Flowerlike Nano-Mg(OH)₂. *ACS Appl. Mater. Interfaces* **2013**, *5*, 9719–9725. [[CrossRef](#)] [[PubMed](#)]
19. Yang, Y.; Zhang, X.; Li, L.; Wei, T.; Li, K. Metastable Dissolution Regularity of Nd³⁺ in Na₂CO₃ Solution and Mechanism. *ACS Omega* **2019**, *4*, 9160–9168. [[CrossRef](#)]
20. Fannin, C.; Edwards, R.; Pearce, J.; Kelly, E. A Study on the Effects of Drying Conditions on the Stability of $\text{NaNd}(\text{CO}_3)_2 \cdot 6\text{H}_2\text{O}$ and $\text{NaEu}(\text{CO}_3)_2 \cdot 6\text{H}_2\text{O}$. *Appl. Geochem.* **2002**, *17*, 1305–1312. [[CrossRef](#)]
21. Biovia, D.S. *Materials Studio 8.0*; Dassault Systèmes: San Diego, CA, USA, 2014.
22. Allen, M.P.; Tildesley, D.J. *Computer Simulation of Liquids*; Oxford University Press: Oxford, UK, 2017; ISBN 0192524704.
23. Anggraeni, A.; Arianto, F.; Mutalib, A.; Pratomo, U.; Bahti, H.H. Fast and simultaneously determination of light and heavy rare earth elements in monazite using combination of ultraviolet-visible spectrophotometry and multivariate analysis. In *AIP Conference Proceedings*; AIP Publishing LLC: Bandung, Indonesia, 2017; Volume 1848, p. 30004. [[CrossRef](#)]
24. Rao, L.; Rai, D.; Felmy, A.R.; Fulton, R.W.; Novak, C.F. Solubility of $\text{NaNd}(\text{CO}_3)_2 \cdot 6\text{H}_2\text{O}$ (c) in Concentrated Na₂CO₃ and NaHCO₃ Solutions. *Radiochim. Acta* **1996**, *75*, 141–148.
25. Jianfeng, Z. Dynamics Simulation of Interaction between Impurity Inhibitors and Aluminum Impurities. In *Ionic Rare Earth Ores No Title*; Jiangxi University of Science and Technology: Jiangxi, China, 2015.